Wideband vibration energy harvester with high permeability magnetic material

X. Xing, J. Lou, G. M. Yang, O. Obi, C. Driscoll, and N. X. Sun[a)]
Department of Electrical and Computer Engineering, Northeastern University, Boston, Massachusetts 02115, USA

(Received 1 June 2009; accepted 4 September 2009; published online 29 September 2009)

A vibration energy harvester based on a high permeability cantilever beam was demonstrated, which overcomes the limitation of the existing approaches in output power and working bandwidth. Magnetostatic coupling between the vibrating highly permeable beam and bias magnetic field leads to maximized flux change and large induced voltage. The coexistence of magnetostatic and elastic potential energy results in the nonlinear oscillation with wide bandwidth. The harvester showed a maximum power of 74 mW and power density of 1.07 mW/cm^3 at 54 Hz under acceleration of 0.57 g (with $g=9.8\ m/s^2$), and bandwidth of 10 Hz (or 18.5% of the operating frequency). © *2009 American Institute of Physics*. [doi:10.1063/1.3238319]

The demand for energy harvesting devices has been growing rapidly with the wide application of mobile electronics and wireless sensors. Mechanical energy associated with vibration has been one of the major energy sources for energy harvesting systems. Different vibration energy harvesting mechanisms have been utilized, including electromagnetic,[1] electrostatic,[2] piezoelectric,[5,6] and magnetoelectric (ME)[3,4] mechanisms. In addition, different functional materials have been applied, such as piezoelectric,[5,6] magnetostrictive,[7,8] and ME composite[4] beams. An electromagnetic microcantilever device with a volume of 0.15 cm^3 was reported to generate a maximum power 46 μW at 52 Hz and an acceleration of 0.59 m/s^2.[1] Optimized electrostatic energy harvesting devices showed an output power 1 mW under vibration amplitude of 90 μm at 50 Hz.[9] Piezoelectric cantilever harvesters were reported to achieve a maximum output power of 790 μW with a tip mass weighing 10 g at the acceleration 9 m/s^2 and frequency 72 Hz, without a coil or magnet.[10] A cantilever of adhesive bonded six layers of magnetostrictive Metglas 2605SC ribbon in a solenoid was claimed to generate a maximum output power of 900 μW at 1 g.[7]

In this work, an alternative vibration energy harvesting model is set up and experimentally verified, based on the strong magnetostatic coupling between the cantilever beam and bias magnet pair. Schematic design of the vibration energy harvester is shown in Fig. 1(a). The key component is a high permeability (high-μ) single layer beam, with one end fixed and the other end vibrating inside a solenoid. Two identical rectangular hard magnets are placed in close proximity to the free end of the high-μ beam outside the solenoid. The bias magnets are aligned in parallel with each other, and the beam. As shown in Fig. 1(b), magnets form a closed flux with their magnetizations antiparallel to each other. When the free end of the cantilever passes through the spatially inhomogeneous magnetic field, the magnetization in the beam is reversed by 180°. The magnetization reversal leads to maximized flux change in the solenoid, resulting in an induced voltage with the same frequency of the mechanical vibrating source. However, when the magnetization of the magnets in parallel, the repulsing magnetic field keeps the beam magnetized toward the same direction all the time. As a result, the magnetic flux change will be smaller in this case, leading to lower output voltage with a frequency that doubles that of the source.

The harvester, including the MuShield® cantilever, the solenoid and a SmCo magnet pair, is seated on a vibrating stage, which is driven by an audio power amplifier connecting to a lock-in amplifier. The mechanical movement of the stage is monitored by an accelerometer. Voltage output of the harvester in time domain is monitored by a digital oscilloscope. Total volume of the energy harvester is 68.96. The coil resistance of the solenoid is 1 Ω, the inductive impedance is 2.86 Ω at 54 Hz, which is obtained by measurement. A lead tip mass is attached on the free end to adjust the vibration amplitude and the intrinsic frequency, which weighs 0.5 g.

Induced voltage across the coil could be predicted by doing intgral along the solenoid because the magnetic field varies along the beam. According to Faraday's law, the open circuit voltage across the coil can be expressed by

$$V_{\text{open}} = \frac{d\phi(t)}{dt} = \frac{d\int \mu_0\{H[x,y(x)] + M[x,y(x,t)]\} \cdot A \cdot dN}{dt} = \frac{d\int \mu_0 M[x,y(x,t)] \cdot A \cdot dN}{dt}, \quad (1)$$

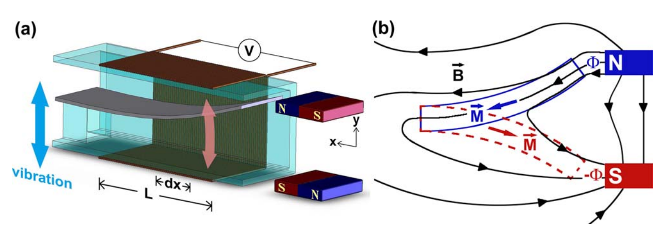

FIG. 1. (Color online) (a) The section view of the schematic design of the vibration energy harvesting device. Dimension of each part is: $4.4\times 3.2 \times 4\ cm^3$ for the solenoid, $1.25\times 2.2\times 1.5\ cm^3$ for the magnet pair including the gap in between, $1.3\times 1.5\times 2.5\ cm^3$ for the mounting frame on one side and $0.5\times 1.5\times 0.6\ cm^3$ on the other. (b) Magnet pair with antiparallel magnetic moment provides maximum magnetic flux change.

a)Electronic mail: nian@ece.neu.edu.

where M is the magnetization in the beam, A is the cross section area of the beam, and dN the number of loops in the infinitesimal length unit of the solenoid dx, shown in Fig. 1(a), and

$$dN = \frac{N_L}{d_w} dx, \tag{2}$$

where N_L is the number of loop layers in the solenoid and d_w is the copper wire diameter. The dimension of the beam is $4.6 \times 0.8 \times 0.0254\ \mathrm{cm}^3$, with a length: width: thickness ratio 181:31.5:1, which makes sure that the length direction is the magnetic easy axis. The magnetic hysteresis loop $M(H)$ along the length direction of the beam was measured in order to calculate the magnetization $M[x,y]$ at an arbitrary point on the beam in the nonuniform magnetic field. Vibration amplitude of an arbitrary point on the beam $y(x,t)$ is got by combining solutions of Euler–Bernoulli beam equation and the equation of motion for the cantilever $a(t)$. According to the Euler–Bernoulli equation and boundary conditions for the cantilever beam, the beam shape function at time t is

$$y(x,t) = a(t)\left(\frac{3Lx^2 - x^3}{2L^3}\right), \tag{3}$$

where L is the length of the beam and $a(t)$ is the amplitude at free end, which is determined by the following equation of motion:

$$m_{\mathrm{eff}} \frac{d^2a(t)}{dt^2} = -\frac{dU}{da} - b\dot{a}(t) + F_{\mathrm{drive}}, \tag{4}$$

where m_{eff} is the effective mass of the beam plus tip mass at the free end, which is 0.74 g. The first term on the right hand side $-dU/da$ is the total force due to the total potential energy,

$$\frac{dU}{da} = \frac{d(U_{\mathrm{magnetic}} + U_{\mathrm{elastic}})}{da}, \tag{5}$$

where the elastic potential energy $U_{\mathrm{elastic}}=(k/2)a^2$, with k the elasticity coefficient which is experimentally determined to be 77 N/m, and U_{magnetic} the magnetic potential due to the bias magnet pair

$$U_{\mathrm{magnetic}} = \int_0^L -\vec{B}[x,y(t)] \cdot d\vec{m}, \tag{6}$$

in which $\vec{m}$ is the magnetic moment in the beam. Size of the identical SmCo hard magnet is $2.2 \times 1.3 \times 0.2\ \mathrm{cm}^3$, providing a fringing magnetic field $\sim$500 Oe at the free end of cantilever and $\sim$10 Oe in the middle of the solenoid. The distribution of magnetic field is obtained with discrete spatial magnetic field measurements and fitted with simulation. The second term $-b\dot{a}$ in Eq. (4) is the mechanical damping term, with b the damping constant which is experimentally determined to be 0.0024 Ns/m. The third term F_{drive} stands for the vibration driving force applied on the fixed end, which is a sine wave input.

Figure 2(a) shows calculated and measured results of the open circuit voltage in two cases. When the magnet pair placed with antiparallel magnetization, the energy harvester shows high open circuit voltage with a peak value 544 mV at a vibration frequency of 54 Hz and acceleration of 0.57 g. As expected, voltage with a doubled frequency 108 Hz and a significantly lowered peak value of 8 mV was observed for the parallel case. It is interesting to note that the mechanical vibration source is a sine wave signal, while the output voltage is not, but with narrow peaks with a full width at half maximum of 1 ms. This is related to the nonuniform magnetic field spatial distribution, leading to the approximate square wave time varying magnetic flux, shown in Fig. 2(b). The free end amplitude dependent flux is also plotted. It is clear that the flux in the beam is reversed immediately while passing the nonstable equilibrium position in the middle, which is the reason for large induced voltage.

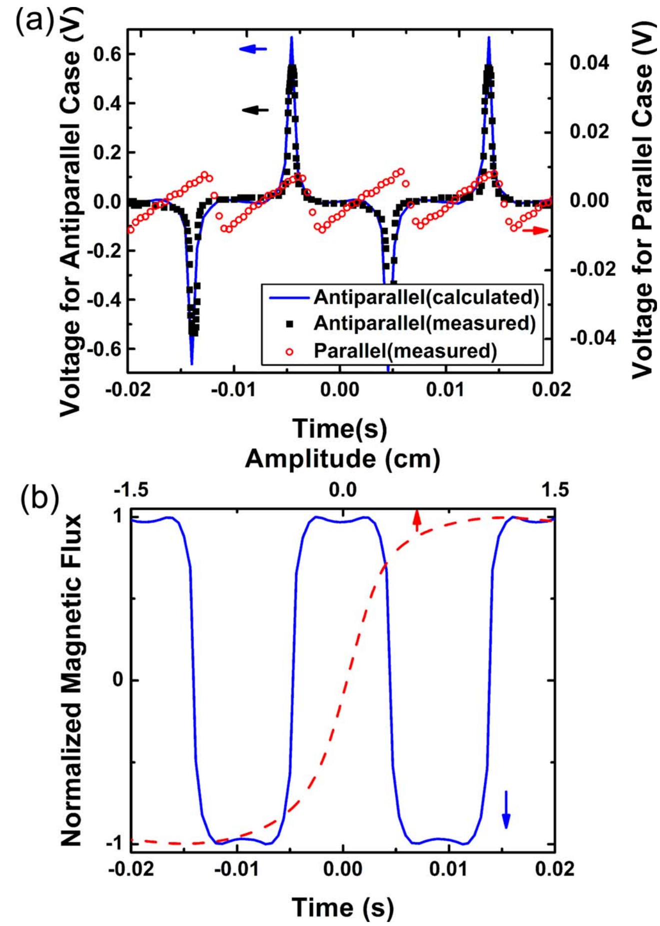

FIG. 2. (Color online) (a) Measured and calculated results of the open circuit voltage for the energy harvesting device at the mechanical vibration frequency 54 Hz, acceleration 0.57 g (g=9.8 m/s^2). (b) Normalized magnetic flux as a function of time and free end amplitude, at vibration frequency 54 Hz, acceleration 0.57 g.

When a load resistance is connected across the coil, the solenoid is equivalent to a resistance in series with an inductance. The output power is optimized when the impedance is matched, $X_L=2\pi fL=X_C=(1/2\pi fC)$ and $R_{\mathrm{load}}=R_{\mathrm{coil}}$, which could be done by inserting a capacitance and adjusting the load resistance. In this way, the maximum output power is

$$P_{\max} = \frac{(V_{\mathrm{open}}/2)^2}{R_{\mathrm{load}}} = \frac{1}{4R_{\mathrm{load}}}\left(A\mu_0 \frac{N_L}{d_w}\right)^2 \left(\int_0^L \left\{\frac{dM[x,y(x,t)]}{dt}\right\} dx\right)^2. \tag{7}$$

Equation (7) indicates that at a particular frequency, the output power depends on the change rate of magnetization in the beam.

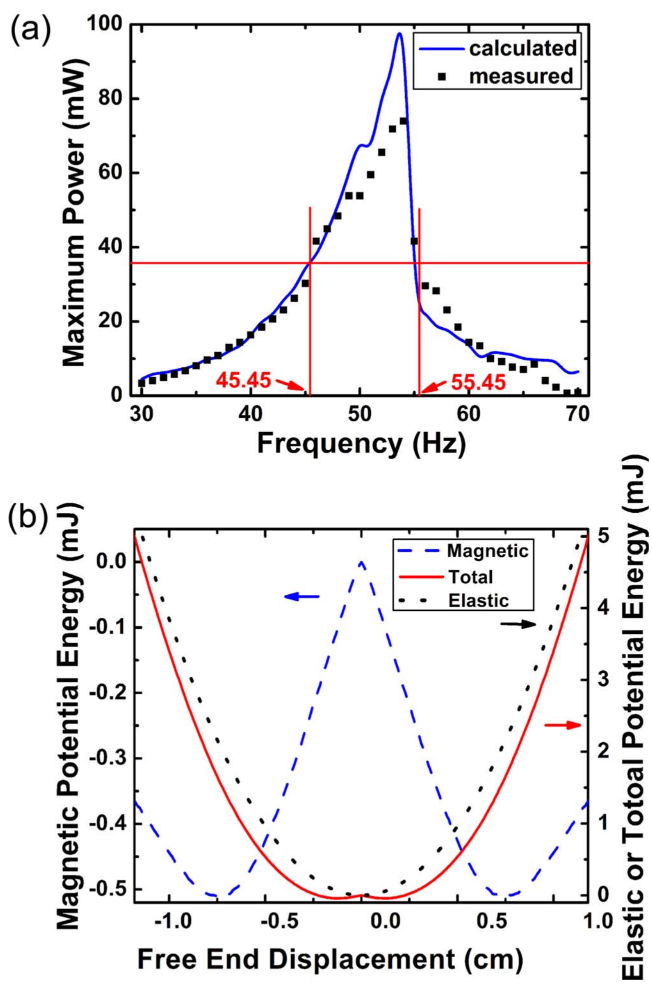

FIG. 3. (Color online) (a) Measured and calculated frequency response of the energy harvester. (b) Elastic potential energy, magnetic potential energy, and total potential energy of the oscillation system as functions of free end displacement of the beam.

Figure 3(a) shows the frequency response. The maximum measured output power is 74 mW on a 1 Ω load and with a time average value 5 mW at an acceleration 0.57 g corresponding to a maximum power density of 1.07 mW/cm^3 or 1.88 $mW/g\ cm^3$. The working bandwidth is about 10 Hz, 18.5% of the central frequency. The major reason for the large bandwidth is the nonlinear dependence of the magnetic force on the displacement of the oscillator.[11] As shown in Fig. 3(b), compared with the elastic potential energy, the magnetic potential energy curve has double potential wells closely connected, resulting in a wider well. As long as the cantilever is supplied with enough energy to get over the potential barrier in the middle, it can vibrate between two wells, a wide oscillation region. However, if the oscillator does not have large enough kinetic energy and is not able to get over the potential barrier, the oscillation is limited in one well. In this case, the behavior of the oscillator is more like that of a linear one, with narrow working bandwidth. Both the calculated and measured curves in Fig. 3(a) exhibit unsymmetrical peaks about the central frequency. This is because the performance of the oscillator at lower band differs from that at higher band. At lower band, it is dominated by nonlinear effect. The output power decreases slowly as the frequency reduced, simply due to the mismatch between the intrinsic and driving source frequency. Even if at a frequency as low as 30 Hz, oscillation between two potential wells was still observed. However, in higher frequency range than 54 Hz, the oscillator was observed trapped in one well, leading to one sided narrow peaks in the voltage signal. This is because in higher frequency range, larger dynamic speed results in larger damping force, so that the cantilever does not have enough energy to climb over the potential barrier in the middle. This single well oscillation dramatically decreases the harvesting efficiency because the cantilever beam can hardly reach flux reversal.

TABLE I. Comparison of key figures of merit for different vibrating energy harvesting mechanisms (a: acceleration; P_d: power density; HPB: half power bandwidth).

Mechanisms/products	f_{center} (Hz)	a (g)	P_{max} (mW)	P_d (mW/cm^3)	HPB (Hz)	Ref.
Electrostatic	50	0.91	1.052	0.58	—	9
Magnetoelectric	40	1	—	0.4	—	4
Piezoelectric	30	1.1	6.5	6.63	—	12
ME sensor based	60	0.1	10.8	0.096	2.1	13
Magnetostrictive	58.1	1	0.2	—	—	7
Perpetuum	21.9	1	92	0.7	12.9	14
KCF	360	0.239	4.1	0.0196	5	15
high-μ	54	0.57	74	1.07	10	—

In summary, an high-μ energy harvesting platform was theoretically studied and tested, which generates a maximum power of 74 mW and density of 1.07 mW/cm^3 at 54 Hz and acceleration of 0.57 g. Wide working bandwidth of 10 Hz or 18.5% of the operating frequency was obtained. Compared with other mechanisms, shown in Table I, this high permeability materials based platform provides great opportunities for energy harvesters that have high power output and wide working bandwidth.

Financial supports from NSF awards 0824008, 0746810 and ONR awards N00014710761, N00014080526 are gratefully acknowledged.

[1]S. P. Beeby, R. N. Torah, M. J. Tudor, P. Glynne-Jones, T. O'Donnell, C. R. Saha, and S. Roy, J. Micromech. Microeng. **17**, 1257 (2007).
[2]S. Roundy, P. K. Wright, and K. Pister, Proceedings of 2002-34309, New Orleans, LA, 17–22 (2002).
[3]J. Huang, R. C. O'Handley, and D. Bono, Proc. SPIE **5050**, 229 (2003).
[4]S. X. Dong, J. Zhai, J. F. Li, D. Viehland, and S. Priya, Appl. Phys. Lett. **93**, 103511 (2008).
[5]S. Roundy, P. K. Wright, and J. Rabaey, Comput. Commun. **26**, 1131 (2003).
[6]N. S. Shenck and J. A. Paradiso, IEEE MICRO **21**, 30 (2001).
[7]L. Wang and F. G. Yuan, Smart Mater. Struct. **17**, 045009 (2008).
[8]X. Zhao and D. G. Lord, J. Appl. Phys. **99**, 08M703 (2006).
[9]G. Despesse, T. Jager, J. Chaillout, J. Leger, and S. Basrour, PRIME **1**, 225 (2005).
[10]R. X. Gao and Y. Cui, Proc. SPIE **5765**, 794 (2005).
[11]F. Cottone, H. Vocca, and L. Gammaitoni, Phys. Rev. Lett. **102**, 080601 (2009).
[12]http://www.mide.com/products/volture/v25w/v25w.php.
[13]http://www.ferrosi.com/files/VEH360_datasheet.pdf.
[14]http://www.perpetuum.co.uk/resource/PMG37%20-%20Technical%20Flyer%20Iss%20C.pdf.
[15]http://www.kcftech.com/products/documents/WSKdatasheet.pdf.